BIOCHEMISTRY
including biophysical chemistry & molecular biology
Article

Biochemistry **2009,** *48,* 7959–7968 7959
DOI: 10.1021/bi900496m

Aromatic Interactions Promote Self-Association of Collagen Triple-Helical Peptides to Higher-Order Structures†

Karunakar Kar,‡ Sajjad Ibrar,‡ Vikas Nanda,‡ Todd M. Getz,§ Satya P. Kunapuli,§ and Barbara Brodsky*,‡

‡*Department of Biochemistry, University of Medicine and Dentistry of New Jersey-Robert Wood Johnson Medical School, Piscataway, New Jersey 08854, and* §*Department of Physiology and Pharmacology, Temple University School of Medicine, Philadelphia, Pennsylvania 19140*

Received March 23, 2009; Revised Manuscript Received July 16, 2009

ABSTRACT: Aromatic residues are relatively rare within the collagen triple helix, but they appear to play a specialized role in higher-order structure and function. The role of aromatic amino acids in the self-assembly of triple-helical peptides was investigated in terms of the kinetics of self-association, the nature of aggregated species formed, and the ability of these species to activate platelet aggregation. The presence of aromatic residues on both ends of a type IV collagen model peptide is observed to greatly accelerate the kinetics of self-association, decreasing the lag time and leading to insoluble, well-defined linear fibrils as well as small soluble aggregates. Both macroscopic visible aggregates and small multimolecular complexes in solution are capable of inducing platelet aggregation through the glycoprotein VI receptor on platelets. Proline−aromatic CH$\cdots\pi$ interactions are often observed within globular proteins and in protein complexes, and examination of molecular packing in the crystal structure of the integrin binding collagen peptide shows Phe interacts with Pro/Hyp in a neighboring triple-helical molecule. An intermolecular interaction between aromatic amino acids and imino acids within the triple helix is also supported by the observed inhibitory effect of isolated Phe amino acids on the self-association of $(Pro\text{-}Hyp\text{-}Gly)_{10}$. Given the high fraction of Pro and Hyp residues on the surface of collagen molecules, it is likely that imino acid−aromatic CH$\cdots\pi$ interactions are important in formation of higher-order structure. We suggest that the catalysis of type I collagen fibrillogenesis by nonhelical telopeptides is due to specific intermolecular CH$\cdots\pi$ interactions between aromatic residues in the telopeptides and Pro/Hyp residues within the triple helix.

The amino acid sequence of collagen is uniquely related to its structure and function. The collagen triple helix is composed of three polypeptide chains, each in an extended polyproline II-like helix, which are supercoiled about a common axis (*1*−*3*). The primary structure of the collagen molecule has a requirement for Gly as every third residue, $(Gly\text{-}Xaa\text{-}Yaa)_n$, generated by the close packing of the three chains near the helix axis. The Gly residues are all buried in the center of the triple helix, while residues in the Xaa and Yaa positions are exposed to solvent. These Xaa and Yaa residues modulate triple-helix stability (*4*) and determine molecular self-association to higher-order structures. A high content of imino acids Pro and hydroxyproline (Hyp, O)[1] in the Xaa and Yaa positions stabilizes the extended polyproline II helix of individual chains, while Hyp confers additional stability through stereoelectronic effects (*5*) and hydration (*2*). In addition to these general amino acid features of collagens, the distribution of charged and hydrophobic residues in the Xaa and Yaa positions in fibril-forming collagens has been correlated with the staggered arrangement of molecules leading to periodic fibrils (*6*, *7*). Aromatic residues are relatively rare within the collagen triple helix, but they appear to play a specialized role in collagen structure and function (*6*, *8*−*11*).

The most well-characterized collagens form axially periodic fibrils, and the most abundant fibrillar collagen is type I, which constitutes the structural backbone of tendon, skin, bone, blood vessels, and cornea (*12*). The process of fibrillogenesis is well-characterized for type I collagen, and the rate of fibrillogenesis increases with an increase in temperature, showing a maximum just below the collagen molecular melting temperature (*13*). Short nonhelical peptides, known as telopeptides, flank the long central triple helix in fibrillar collagens. These telopeptides are unusually rich in Tyr and Phe and have been shown to catalyze the process of fibril formation (*9*−*11*). It was noted some years ago that Phe residues within type I collagen are aligned in the gap region of the fibril, and it was proposed that Phe−Phe interactions confer rigidity and stability to this more flexible region of the fibril (*6*, *14*).

Collagen model peptides have proven to be capable of self-assembly into higher-order structures and offer an approach to relating amino acid sequence with the self-association of triple-helical molecules (*15*−*23*). The process of self-assembly of the model peptide $(Pro\text{-}Hyp\text{-}Gly)_{10}$ was found to have many

†This work was supported by National Institutes of Health (NIH) Grant GM60048 (B.B.) and NIH Grant HL81321 (S.P.K.). S.I. was supported by the RISE (Research In Science and Engineering) at the Rutgers/UMDNJ summer program, jointly sponsored by the Graduate School of Biomedical Sciences at RWJMS and the Rutgers Graduate School-New Brunswick.

*To whom correspondence should be addressed: Department of Biochemistry, UMDNJ-Robert Wood Johnson Medical School, 675 Hoes Lane, Piscataway, NJ 08854. Telephone: (732) 235-4397. Fax: (732) 235-4783. E-mail: brodsky@umdnj.edu.

[1]Abbreviations: CD, circular dichroism; DSC, differential scanning calorimetry; DLS, dynamic light scattering; GPVI, glycoprotein VI; PDB, Protein Data Bank. The residue hydroxyproline is represented by Hyp in the three-letter code and O in the one-letter code. Peptides are designated as T4 for $(POG)_3QOGLOGLOG(POG)_4$, T4Y for $(GPO)_3GQOGLOGLO(GPO)_4GY$, FT4Y for $F(GPO)_3GQOGLOGLO(GPO)_4GY$, and $(POG)_{10}$ for $(Pro\text{-}Hyp\text{-}Gly)_{10}$.

Published on Web 07/18/2009

similarities to the process of collagen fibril formation, in terms of its dependence on temperature, pH, and solvent, but the (Pro-Hyp-Gly)$_{10}$ self-association has a much higher critical concentration than collagen and did not form the highly ordered periodic structures seen for collagen (*17*). Inclusion of a selected distribution of charged residues in a collagen peptide led to the formation of large banded fibrils (*21*), while inclusion of hydrophobic sequences led to fibrillar structures, some with supercoiled and branching features like those found in basement membrane networks (*23*). These results suggest triple-helical peptides may have common interactions involving hydration and hydroxyproline (Hyp, O) that promote nonspecific self-association, but that charged and hydrophobic interactions confer specificity and a high affinity for self-association. Recently, addition of aromatic residues to the ends of triple-helical peptides has been shown to accelerate the self-association process and to increase the order and size of the final aggregates (*15*, *16*).

Triple-helical peptides have also proven to be valuable in probing collagen interactions leading to biological activity (*8*). The information gained about peptide self-association to higher-order structures may be used to probe the role of aggregates of triple-helical molecules in biological processes. For example, a nonaggregated triple-helical form of the peptide, e.g., (Pro-Hyp-Gly)$_{10}$, is not sufficient for activation of platelet aggregation, while a disulfide cross-linked higher-order molecular form of the same peptide, designated CRP (collagen reactive peptide), is a strong inducer of platelet aggregation (*24*). CRP binds and activates the same glycoprotein VI (GPVI) tyrosine kinase receptor that responds to collagen, triggering a signal cascade that results in platelet aggregation (*25*). Recent peptide studies from the Farndale laboratory showed that at least two sequential Gly-Pro-Hyp sequences are necessary to activate platelets and that peptides containing specific type III collagen sequences can bind to platelets and induce aggregation (*25*, *26*). Large fibrils formed from non-cross-linked (Pro-Hyp-Gly)$_{10}$ peptides capped by aromatic residues on both ends were observed to be good activators of this process (*15*, *16*). The precise nature of the triple-helical peptide aggregate required to induce platelet activation is not well-defined.

Here, investigation of the role of aromatic amino acids in the self-assembly of triple-helical peptides is extended to characterize the kinetics of self-association, the nature of aggregated species, and the ability of different species to induce platelet activation. The presence of aromatic residues on both ends of a type IV collagen model peptide is observed to result in marked acceleration of aggregation and a decreased lag time, leading to insoluble, well-defined linear fibrils as well as small soluble aggregates. Both macroscopic visible aggregates and small soluble multimolecular assemblies are capable of inducing platelet aggregation through the glycoprotein VI receptor on platelets. CH$\cdots\pi$ interactions between imino acids within the triple helix and aromatic residues are suggested by the inhibitory effect of isolated Phe amino acids on the self-association of (Pro-Hyp-Gly)$_{10}$ and by an analysis of a high-resolution crystal structure of a collagen peptide containing Phe. The relevance of these studies with respect to triple-helical model peptides for collagen fibrillogenesis is considered.

EXPERIMENTAL PROCEDURES

Peptides. A typical sequence from the α5 chain of type IV collagen (residues 491−499) including Hyp at every Yaa position and several hydrophobic residues was selected as described previously (*23*). The peptides were synthesized by Tufts University Core facility (Boston, MA): (POG)$_3$QOGLOGLOG-(POG)$_4$, denoted as T4; (GPO)$_3$GQOGLOGLO(GPO)$_4$GY, denoted as T4Y; and F(GPO)$_3$GQOGLOGLO(GPO)$_4$GY, denoted as FT4Y. Peptides were purified on a C-18 column using a reverse-phase HPLC system (Shimadzu), and the purity was ensured by mass spectrometry using MALDI-TOF (DE-PRO mass spectrometer). The (Pro-Hyp-Gly)$_{10}$ peptide was obtained from Peptides International (Louisville, KY). For peptides having Tyr residues, the peptide concentration was determined using an extinction coefficient (ε_{280}) of 13980 M^{-1} cm^{-1} (*27*). Concentrations of the peptides without Tyr were measured by monitoring the absorbance at 214 nm using an ε_{214} of 2200 cm^{-1} M^{-1} per peptide bond. Two buffers were used: 20 mM PBS buffer (10 mM NaH_2PO_4, 10 mM Na_2HPO_4, and 150 mM NaCl) for pH 7 and acetate buffer (20 mM with 150 mM NaCl) for pH 3. Amino acids L-phenylalanine, L-leucine, L-alanine, L-histidine, and L-tyrosine were purchased from Sigma.

Turbidity Measurements. Turbidity curves monitoring the process of self-assembly of collagen peptides were obtained using the optical density at 313 nm as a function of time on a Beckman DU 640 spectrophotometer with a Peltier temperature controller. A peptide solution of 600 μL was kept in a 5 mm cell sealed to avoid evaporation and then subjected to the desired constant temperature.

Circular Dichroism Spectroscopy. Circular dichroism (CD) measurements were taken using an Aviv model 62DS spectrophotometer (Aviv Biomedical, Inc.). Prior to CD measurements, each sample was incubated at 4 °C for 2−3 days to allow the formation of triple helix. The characteristic triple-helix CD maximum at 225 nm was used to monitor thermal transitions (*28*).

Electron Microscopy. Electron microscopy was conducted on negatively stained samples of peptide aggregates to visualize the morphology of the higher-order structures. A small aliquot of the sample was placed on a 400-mesh carbon-coated copper grid, air-dried, and stained with uranyl acetate for 10 s. Specimens were examined with a transmission electron microscope using a Phillips 420 instrument.

Dynamic Light Scattering. DLS measurements were performed using a DynaPro Titan instrument (Wyatt Technology Corp., Santa Barbara, CA) equipped with a temperature controller using a 12 μL quartz cuvette. All samples were centrifuged and filtered through 0.1 μm Whatman Anotop filters before measurements. To obtain the hydrodynamic radii (R_h), the intensity autocorrelation functions were analyzed with Dynamics software (Wyatt Technology Corp.). For data analysis, a viscosity ($\eta_{20\ °C}$) value of 1.019 cP was used for PBS.

Differential Scanning Calorimetry. Differential scanning calorimetry (DSC) measurements were performed on a Nano-DSC II, model 6100 scanning calorimeter from Calorimetry Sciences Corp. All DSC profiles were obtained at a scan rate of 1 °C/min, and each curve was baseline subtracted before data analysis. Prior to all measurements, peptide solutions were dialyzed. ΔH_{cal} values were obtained by integrating the excess heat capacity curve.

Structure Analysis. The crystal structure of the GFOGER collagen model peptide, with the sequence GPOGPOGFO-GERGPOGPOGPO, which binds to the α2β1 integrin (PDB entry 1Q7D) (*29*), was analyzed to characterize molecular packing around Phe9. Structures in the unit cell were generated using the "Build Crystallographic Symmetry" function of DeepView

Table 1: List of Type IV Collagen Model Peptide Sequences, Melting Temperatures (T_m), Calorimetric Enthalpies (ΔH_{cal}), Self-Association Times at the Optimal Incubation Temperature, and Their Effect on Platelet Activation[a]

						$t_{1/2}$ of self-assembly[f]		activation of platelets	
peptide	sequence	T_m (°C)[b]	ΔH_{cal} (kJ/mol)[c]	R_h[d] (nm)	critical concentration[e] (mg/mL)	c = 7 mg/mL	c = 3 mg/mL	soluble state[g]	aggregated state[h]
T4	$(POG)_3QOGLOGLOG(POG)_4$	41.3	259	2.0	5.9	~24 h	> 48 h	−	+
T4Y	$(GPO)_3GQOGLOGLO(GPO)_4$**GY**	44.0	287	2.2, 31.0	3.4	~3 min	> 48 h	+	+
FT4Y	**F**$(GPO)_3GQOGLOGLO(GPO)_4$**GY**	48.0	284	2.5, 33.5	1.4	< 1 min	~3 min	+	+
$(POG)_{10}$	$(POG)_{10}$	58.8	390	1.9	2.0	~3 min	> 12 h	−	−

[a] Values for $(Pro\text{-}Hyp\text{-}Gly)_{10}$ are given as a control. [b] The T_m values reported here were obtained from overnight melting experiments using CD at a sample concentration of 1 mg/mL in PBS buffer at pH 7 (*28*). [c] Calorimetric enthalpy values were obtained by thermal unfolding of triple-helical peptides using DSC, at 1 mg/mL in PBS (pH 7) with a scan rate of 1 °C/min. [d] Hydrodynamic radii of the molecular species were measured at 4 °C by using DLS, at 1 mg/mL PBS (pH 7) in the soluble state. R_h values mentioned here represent the average values of at least five measurements. [e] Critical concentrations were determined using a spectrophotometer to analyze the concentration of the supernatant of the aggregated samples after the plateau phase was reached. [f] $t_{1/2}$ values for the self-assembly process for the peptides were obtained from turbidity curves considering the time taken to reach the half-value of the maximum turbidity rise at a temperature ~2 °C below the T_m value. [g] The concentration of the soluble samples was studied at 200 μg/mL for all the peptides. [h] Solutions of peptides were prepared at 7 mg/mL for $(Pro\text{-}Hyp\text{-}Gly)_{10}$, T4, and T4Y in PBS (pH 7) and kept at 4 °C for 2 days. Aggregation was achieved by incubation at their respective optimal temperatures: 58 °C overnight for $(Pro\text{-}Hyp\text{-}Gly)_{10}$, 44 °C overnight for T4Y, and 40 °C for 2 days for T4. For the FT4Y peptide, the concentration was 3 mg/mL and the sample was incubated overnight at 47 °C for aggregation.

version 4.0 (www.expasy.org/spdbv), using the *C*2221 space group.

Platelet Aggregation Studies. Apyrase (type VII), indomethacin, P2Y1 antagonist MRS 2179, and P2Y12 antagonist AR-C69931 were obtained from Sigma (St. Louis, MO). Convulxin was purchased from Centerchem (Norwalk, CT). Primary antibody Syk (4D10) was obtained from Santa Cruz Biotechnology (Santa Cruz, CA) and phospho-Syk Tyr525/526 from Cell Signaling Technologies (Beverly, MA). LI-COR Odyssey blocking buffer and secondary antibodies goat anti-rabbit IRDye 800CW and goat anti-mouse IRDye 680 were purchased from LI-COR Biosciences (Lincoln, NE). Whatman protran nitrocellulose transfer membrane was obtained from Fisher Scientific (Pittsburgh, PA).

Whole blood was drawn from healthy, consenting human volunteers into tubes containing one-sixth volume of ACD (2.5 g of sodium citrate, 1.5 g of citric acid, and 2 g of glucose in 100 mL of deionized water) and centrifuged at 230*g* for 20 min at room temperature to yield PRP (platelet-rich plasma). The PRP was then centrifuged at 980*g* for 10 min at room temperature to pellet the platelets. Platelets were resuspended in Tyrode's buffer [138 mM NaCl, 2.7 mM KCl, 1 mM $MgCl_2$, 3 mM NaH_2PO_4, 5 mM glucose, and 10 mM Hepes (pH 7.4)] containing 0.2 unit/mL apyrase. Cells were counted using a Coulter Z1 Particle Counter, and the concentration of cells was adjusted to 2×10^8 platelets/mL. All experiments using washed platelets were performed in the absence of extracellular calcium.

Aggregation of 0.5 mL of washed platelets was analyzed using a PICA lumi aggregometer (Chrono-log). Platelets were activated with varying concentrations of collagen peptides or 100 ng of convulxin. To examine the effect of peptides in their associated forms, the peptides $(Pro\text{-}Hyp\text{-}Gly)_{10}$ (7 mg/mL), T4 (7 mg/mL), T4Y (7 mg/mL), and FT4Y (3 mg/mL) were incubated at their respective optimal temperatures to promote self-association. After turbidity reached the plateau phase, aggregated peptide samples were incubated in a platelet activation assay at 37 °C. The dose-dependent platelet activation by FT4Y peptide (3 mg/mL, PBS) was assessed by adding different volumes (1−35 μL) of the turbid peptide sample of FT4Y to 500 μL of platelet suspension and assessing aggregation using light transmission while stirring (900 revolutions/min) at 37 °C. Aggregation tracings are representative of results obtained from three separate experiments on three different donors. Experiments are also conducted in the presence of P2Y1 receptor antagonist MRS 2179, P2Y12 receptor agonist AR-C69931, and indomethacin which were added just prior to the addition of agonist.

For Western blot analysis, platelets were stimulated for 30 s while being stirred with varying concentrations of FT4Y peptide or 100 ng of convulxin as a control. The reaction was stopped by the addition of 6.6 N perchloric acid, and the resulting acid precipitate was collected and chilled on ice. The pellets were centrifuged at 13000*g* for 10 min, followed by rinsing and subsequent resuspension in 0.5 mL of deionized water. The protein was again pelleted by centrifugation at 13000*g* for 10 min. The protein pellets were solubilized in sample buffer containing 2 M Tris, 10% SDS, glycerol, 0.5% bromophenol blue, and 100 mM DTT and then boiled for 10 min. Bovine skin collagen was also used as a control.

Samples were subjected to SDS−PAGE on 10% polyacrylamide gels. Proteins were transferred to a Whatman Protran nitrocellulose membrane, blocked with Odyssey blocking buffer for 1 h, and incubated overnight at 4 °C with primary antibody anti-Syk (4D10) and anti-phospho-Syk525/526 (1:1000 in Odyssey blocking buffer) with gentle agitation. After four washes for 5 min each with PBS-T, the membranes were probed with Li-Cor Odyssey goat anti-rabbit IRDye 800CW and goat anti-mouse IRDye 680 (1:1000 in PBS-T) for 1 h at room temperature (23 °C). After four washes for 5 min each with PBS-T and one wash in deionized water, membranes were examined with a Li-Cor Odyssey infrared imaging system.

RESULTS

Self-Association and Platelet Activation by a Type IV Collagen Model Peptide with Aromatic Residues on Both Ends. The effect of having aromatic residues on no ends, one end, or both ends of a collagen model peptide was investigated in terms of the kinetics of self-association, the aggregated species formed, and the ability of all species to activate platelet aggregation. A collagen model peptide denoted as T4 contains a central hydrophobic sequence GPOGQOGLOGLOGPO from the α5 chain of type IV collagen (residues 491−499) flanked by (Gly-Pro-Hyp) triplets. The peptide was previously studied with no aromatic residues and with a C-terminal Tyr residue (*23*), and

here these are compared with a new construct capped by an N-terminal Phe residue as well as a C-terminal Tyr, designated as peptide FT4Y (Table 1). CD spectroscopy indicates that peptide FT4Y forms a triple helix with a thermal stability (T_m) of 48 °C which is higher than that seen for the homologous peptide with only a C-terminal Tyr (T_m = 44 °C) or no aromatic residues (T_m = 41 °C). Differential scanning calorimetry (DSC) of FT4Y at 1 mg/mL shows a single thermal transition at a higher temperature, 55.5 °C, consistent with the faster heating rate for the DSC (1 °C/min) compared with CD (0.1 °C/min) under nonequilibrium conditions (*28*). The FT4Y calorimetric enthalpy is 284 kJ/mol, compared to 287 and 259 kJ/mol for T4Y and T4, respectively, at 1 mg/mL, suggesting similar hydrogen bonding and hydration (Table 1).

The presence of a single tyrosine residue at the C-terminal end of the triple helix was previously shown to greatly accelerate peptide self-association (*23*), with $t_{1/2}$ decreasing from ~24 h for T4 to ~3 min for T4Y (c = 7 mg/mL, ~2 °C below the T_m). The additional N-terminal Phe in FT4Y increased the rate of self-assembly so much that aggregates were formed before the sample could be monitored by turbidity at 7 mg/mL (Table 1). When the FT4Y concentration was reduced to 3 mg/mL, lag, growth, and plateau phases were observed (Figure 1a), while neither T4Y nor T4 shows any aggregation at this concentration within 48 h. The self-association of FT4Y (c = 3 mg/mL) was temperature-dependent, with an optimum near 46 °C (Figure 1b), consistent with previous observations that showed that the optimal rate of peptide self-association is several degrees below its T_m value (*17*, *23*). Centrifugation of the suspension indicates a critical concentration of ~1.4 mg/mL for FT4Y, a value lower than those seen for T4Y (3.4 mg/mL) and T4 (5.9 mg/mL) (Table 1). Under aggregating conditions (3 mg/mL, PBS, pH 7), the DSC profile of FT4Y shows two distinct peaks (Figure 1c). The first transition at 55.5 °C corresponds to the melting of triple-helical molecules into unfolded chains, while the second smaller transition at 88.7 °C corresponds to a loss of turbidity and is likely to reflect dissociation of higher-order structures formed during the DSC scan (*17*).

To visualize the structures formed as result of self-association, negatively stained samples of FT4Y were observed by electron microscopy (Figure 2). The micrographs show linear fibrillar structures with diameters ranging from 20 to 40 nm. In some cases, it appears that two fibrillar units are twisted around each other. There is no indication of axial banding. These structures looked similar to the higher-order structures reported previously for T4Y and T4 (*23*).

Dynamic light scattering (DLS) studies were conducted with peptides T4, T4Y, and FT4Y to determine translational diffusion constants and characterize homogeneity and aggregation (Figure 3). At low temperatures (c = 7 mg/mL), peptide T4 shows only one peak with a hydrodynamic radius (R_h) of ~2 nm, a value close to that reported previously for a single trimer molecular species of $(Pro\text{-}Hyp\text{-}Gly)_{10}$ and other triple-helical peptides similar in length (*17*) (Table 1). The presence of an aromatic residue on one end or both ends of the T4 peptide is observed to lead to formation of soluble multimolecular species. The DLS profiles of peptides T4Y and FT4Y at low temperatures (c = 1 and 3 mg/mL) show a higher-molecular weight peak with an R_h of ~32 nm in addition to the single triple-helical molecular species with R_h values of ~2.1 and ~2.5 nm, respectively. An increasing temperature leads to a decrease in the intensity of the 2.5 nm peak and corresponding increase in the intensity of the ~32 nm peak, until the temperature reaches ~46 °C, where

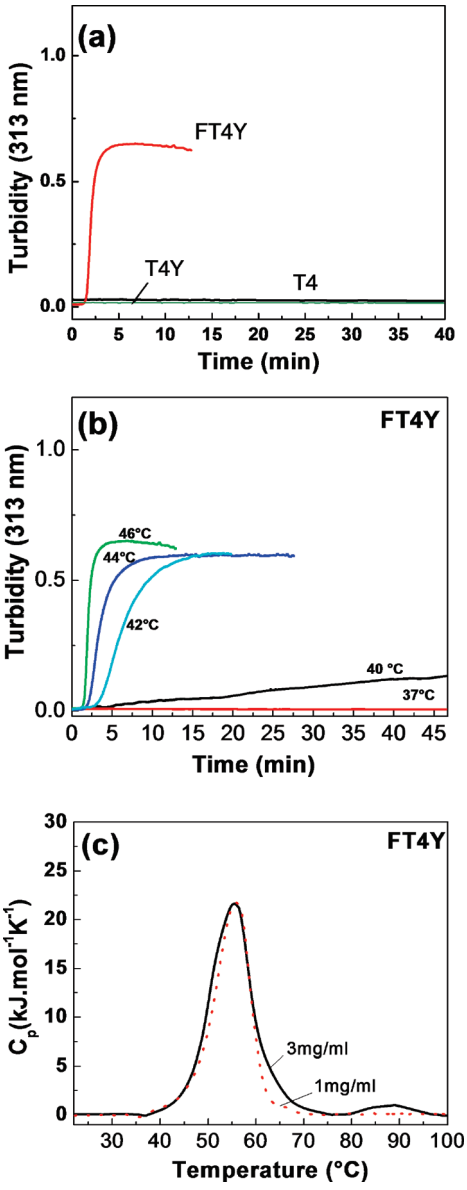

FIGURE 1: (a) Turbidity curves for the self-assembly of type IV collagen model peptides (c = 3 mg/mL) as measured by monitoring the rise in absorbance at 313 nm: FT4Y (incubation temperature of 46 °C), T4Y (incubation temperature of 44 °C), and T4 (incubation temperature of 41 °C). (b) Turbidity curves for peptide FT4Y showing the temperature dependence of the self-assembly process (3 mg/mL, PBS, pH 7). (c) DSC profile of the thermal unfolding of FT4Y (pH 7, PBS) at the aggregating concentration [3 mg/mL (—)] and the nonaggregating concentration [1 mg/mL (···)] with a heating rate of 1 °C/min.

turbidity and visible aggregation prevent collection of DLS data (Figure 3e). When the 46 °C aggregated sample is cooled to 4 °C, the visible aggregates disappear and become completely soluble, while the trimer species (R_h ~ 2.5 nm) and the larger molecular species (R_h ~ 32 nm) are present again, indicating reversibility of the association process.

Peptides $(Pro\text{-}Hyp\text{-}Gly)_{10}$, T4, T4Y, and FT4Y in soluble and aggregated states were tested for their ability to induce platelet aggregation. There was no platelet activation by either the soluble form of $(Pro\text{-}Hyp\text{-}Gly)_{10}$ or its temperature-induced clumplike aggregated structure. The fibrous forms of peptides T4, T4Y, and FT4Y and the soluble forms of FT4Y and T4Y which contained multimolecular species did induce activation of platelet aggregation,

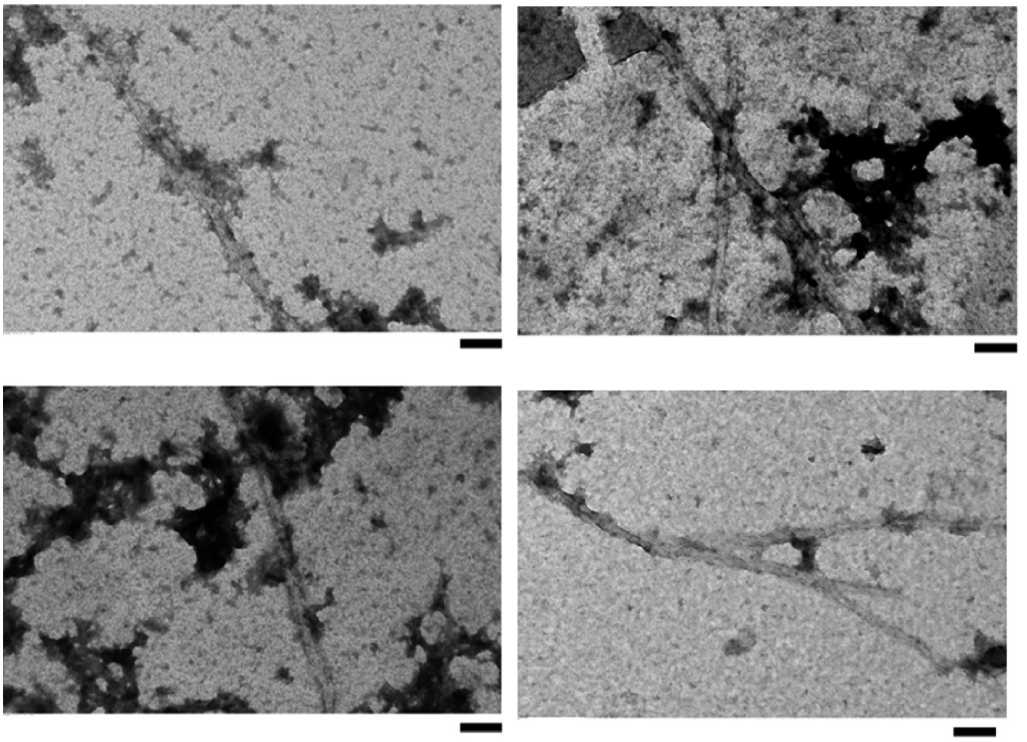

FIGURE 2: Panel of four representative electron micrographs of negatively stained samples of the visibly aggregated form of FT4Y peptide (c = 3 mg/mL, pH 7), following incubation at 46 °C for 6 h to induce self-assembly. The scale bar is 100 nm.

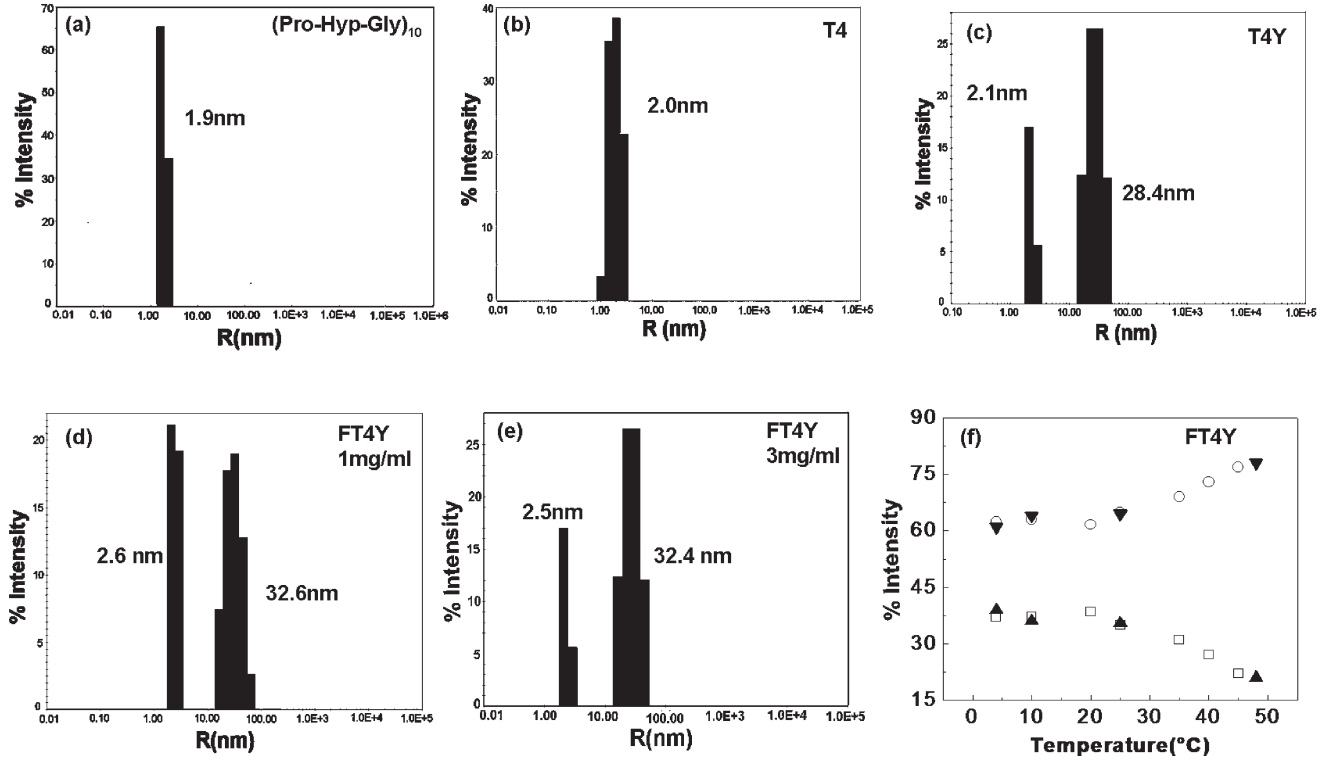

FIGURE 3: Dynamic light scattering analysis of triple-helical peptides in PBS buffer at pH 7 and 4 °C, showing the hydrodynamic radii (R_h) generated from the data: (a) $(Pro\text{-}Hyp\text{-}Gly)_{10}$ (c = 7 mg/mL), (b) T4 (c = 7 mg/mL), (c) T4Y (c = 7 mg/mL), (d) FT4Y (c = 1 mg/mL), and (e) FT4Y (c = 3 mg/mL). In panel f, the changes in the percent intensity of the trimer species ($R_h \sim 2.5$ nm) and oligomeric species ($R_h \sim 32$ nm) of peptide FT4Y are shown as a function of temperature for two concentrations: (□) 2.5 nm peak at 3 mg/mL, (○) 32 nm peak at 3 mg/mL, (▲) 2.5 nm peak at 1 mg/mL, and (▼) 32 nm peak at 1 mg/mL. The R_h values given in Table 1 represent the mean values of five to six measurements taken from DLS data.

displaying activation similar to that of a convulxin control and bovine skin collagen (data not shown). In contrast, the soluble form of peptide T4 with only trimer species did not induce activation. The effect of FT4Y aggregates on platelet functional responses was characterized in detail. The visible aggregates of FT4Y activated platelets in a concentration-dependent manner. At low concentrations (3 μg/mL), the FT4Y peptide induced platelet shape change, while increasing concentrations caused full

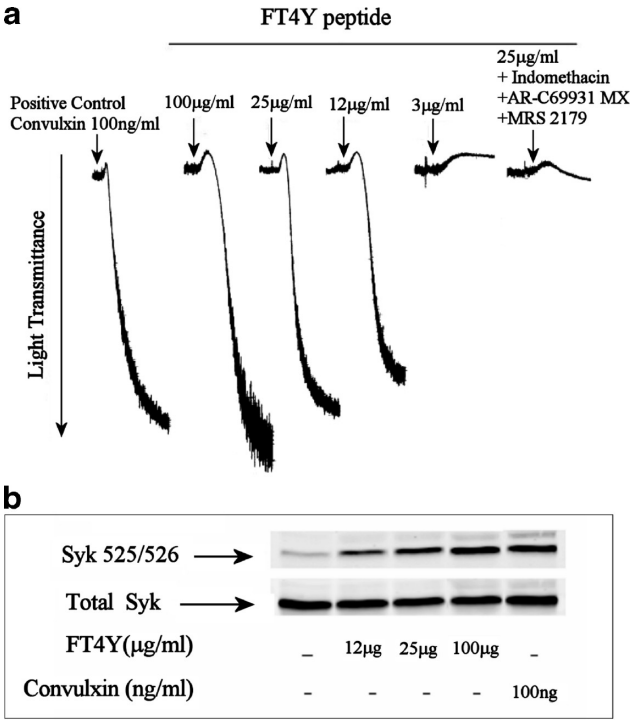

FIGURE 4: Activation of platelet aggregation by FT4Y. (a) Washed human platelets were stimulated with different doses (3−100 μg/mL) of the aggregated FT4Y sample at 37 °C in the aggregometer. Convulxin (100 ng/mL) was taken as a positive control. The effect of platelet activation by FT4Y (25 μg) was examined in the presence of indomethacin (100 nM), AR-C69931 (100 nM), and MRS 2179 (100 μM). (b) Western blot showing the phosphorylation of the Syk protein at different doses of the FT4Y peptide. The data are representative of at least three experiments using platelets from different donors.

platelet aggregation (Figure 4). In the presence of the thromboxane inhibitor indomethacin, and ADP receptor antagonists ARC-69931MX and MRS 2179 (*30*), platelets failed to aggregate in response to FT4Y, indicating a dependence of the process on positive feedback from thromboxane and secreted ADP. The ability of FT4Y to activate GPVI pathways was supported by the concentration-dependent phosphorylation of Syk on tyrosine residues 525 and 526 (*31*, *32*) (Figure 4b).

Interactions of Phe with Triple-Helical Peptides. To further investigate the interactions between aromatic residues and triple helices, the effect of isolated Phe residues on the aggregation process of collagen model peptides was characterized. Monitoring the self-association of $(Pro\text{-}Hyp\text{-}Gly)_{10}$ (c = 7 mg/mL, 58 °C) by turbidity indicates the addition of Phe (peptide:Phe molar ratio of 1:60) leads to a significantly longer lag time, a decreased rate of growth, and a decreased magnitude of the maximal height in the plateau phase (Figure 5a). Addition of isolated Leu or Ala amino acids has no effect on the self-assembly of $(Pro\text{-}Hyp\text{-}Gly)_{10}$ at the same concentrations, indicating the importance of the aromatic nature of the amino acid (Figure 5a). The presence of Phe also led to a substantial delay in self-association for peptides T4Y (c = 7 mg/mL, 44 °C) (Figure 5b) and FT4Y (c = 3 mg/mL, 46 °C) (data not shown).

Since Phe interfered with the self-assembly of $(Pro\text{-}Hyp\text{-}Gly)_{10}$ and other triple-helical peptides, the possibility of direct binding of the isolated amino acid Phe to $(Pro\text{-}Hyp\text{-}Gly)_{10}$ was investigated. Isothermal titration calorimetry experiments were not successful because of strong signals from Phe residues in solution,

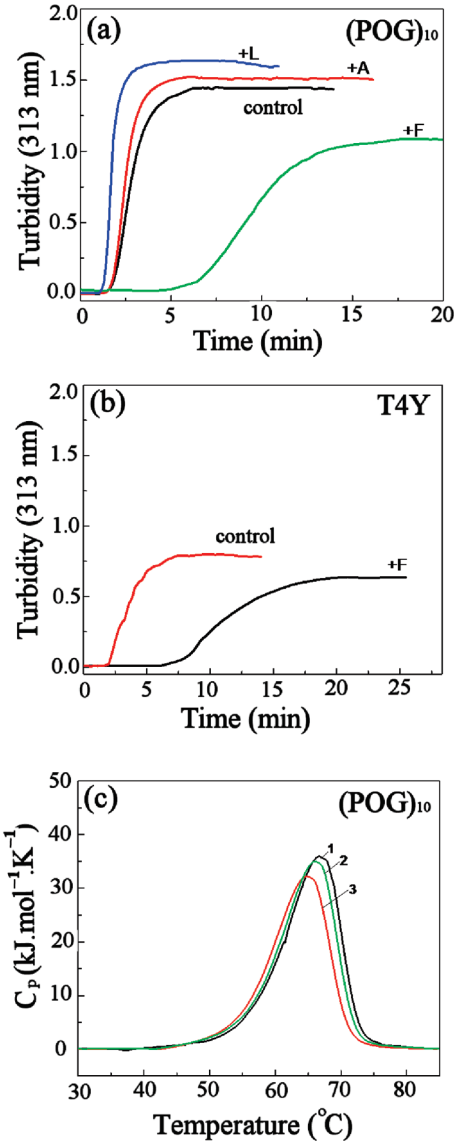

FIGURE 5: Effect of addition of isolated phenylalanine to the sample solution on the self-assembly of triple-helical peptides as measured by the rise in turbidity at 313 nm. (a) Self-assembly of $(Pro\text{-}Hyp\text{-}Gly)_{10}$ (c = 7 mg/mL, PBS, 58 °C): $(Pro\text{-}Hyp\text{-}Gly)_{10}$ only (control), $(Pro\text{-}Hyp\text{-}Gly)_{10}$ with Phe (1peptide:60F), $(Pro\text{-}Hyp\text{-}Gly)_{10}$ with Ala (1peptide:60A), and $(Pro\text{-}Hyp\text{-}Gly)_{10}$ with Leu (1peptide:60 L). (b) Turbidity curves for T4Y peptide assembly (c = 7 mg/mL, PBS, 44 °C): T4Y only (control) and T4Y with Phe (1peptide:60F). (c) DSC profiles of thermal unfolding of triple-helical peptide $(Pro\text{-}Hyp\text{-}Gly)_{10}$ (c = 1 mg/mL, PBS, pH 7) in the presence and absence of Phe: (1) $(Pro\text{-}Hyp\text{-}Gly)_{10}$ only, (2) $(Pro\text{-}Hyp\text{-}Gly)_{10}$ with Phe (1:60), and (3) $(Pro\text{-}Hyp\text{-}Gly)_{10}$ with Phe (1:200). Phe was chosen because of its high solubility in PBS buffer, in contrast to the insolubility of Tyr.

which could result from aromatic stacking or solvation. Differential scanning calorimetry (DSC) measurements of $(Pro\text{-}Hyp\text{-}Gly)_{10}$ (PBS, pH 7, c = 1 mg/mL) showed a slight destabilization in the presence of high concentrations of Phe (peptide:Phe molar ratio of 1:200) (Figure 5c).

Analysis of Aromatic Residue Interactions in the High-Resolution Structure of a Collagen Peptide. The interactions of Phe residues in triple-helical molecules were explored using the high-resolution structure of the collagen model peptide that binds $\alpha 2\beta 1$ integrin (PDB entry 1Q7D) (*29*). This peptide sequence contains one Phe residue at position 9 in the middle of the triple helix (GPOGPOGFOGERGPOGPOGPO), and the crystal

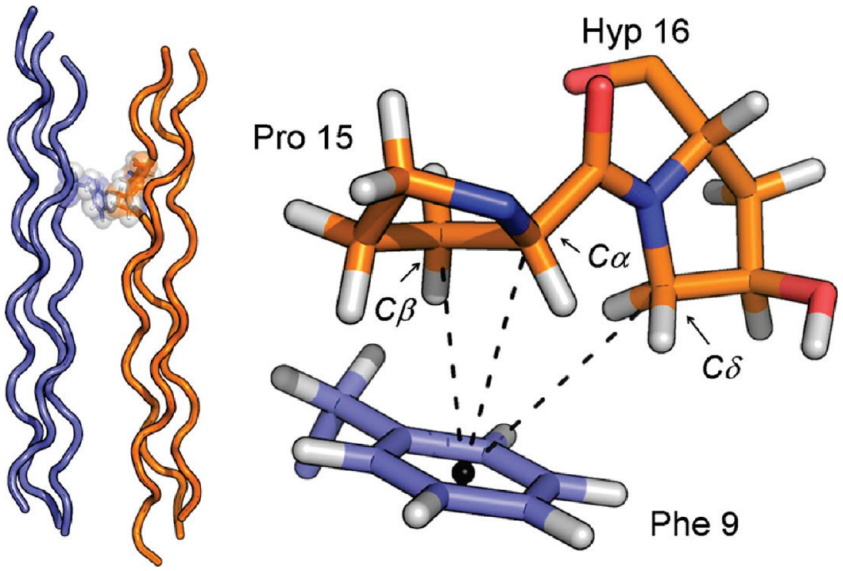

FIGURE 6: On the left is a portion of the unit cell of the GFOGER integrin binding peptide (PDB entry 1Q7D) showing two antiparallel triple helices and the location of the Phe9 residue on the blue molecule. On the right is a close-up view of Phe9 participating in CH···π interactions with Pro15 and Hyp16 (see the text for details about the geometry). Dashed lines represent hydrogen bonds from the imino acid carbon donor to the center of the aromatic ring. Hydrogen coordinates are modeled using ideal bond angles and lengths. The best interaction geometry is for Phe9 with Pro15 Cβ, with a $d_{C\beta\cdots R}$ of 3.72 Å and a $\theta_{C\beta-H\cdots R}$ of 143°.

packing shows a distorted hexagonal arrangement of triple helices with an average axis−axis distance of 14 Å. The Phe residue, in the Xaa position of the triple helix, does not interact with any residues within the same molecule, but examination of Phe environments in the unit cell shows a significant number of intermolecular contacts (Figure 6). CH···π interactions between Phe and imino acids are observed between an antiparallel pair of triple helices (Figure 6). The Cδ atom of Hyp16 together with the Cα atom and the Cβ atom of Pro15 participate in a network of CH···π hydrogen bonds with Phe9 across a crystal packing interface. The distance and angles between the Phe and the Cβ and Cα atoms of Pro15 satisfy the criteria defined by Brandl et al. (*33*) for CH···π hydrogen bonds ($d_{C\beta\cdots R}$ < 4.5 Å; $\theta_{C\delta-H\cdots R}$ between 120° and 180°), while the Hyp16 Cδ interaction falls slightly outside the angle constraint. At the parallel crystal packing interface between a pair of triple helices in the GFOGER peptide unit cell, Phe9 on one triple-helix molecule is in the vicinity of an equivalent Phe on another molecule, but the aromatic ring center−center distance of 7.6 Å precludes any possibility of $\pi-\pi$ stacking or other commonly observed aromatic−aromatic interaction motifs (*34*). In this parallel pair of triple helices, the Phe does make an interchain edge−edge contact with Hyp10, but this does not satisfy the geometric criteria for a CH···π hydrogen bond (*33*).

DISCUSSION

Aromatic Residue Interactions and Association of Triple-Helical Peptides. The studies reported here provide new information about interactions of aromatic amino acids in the context of collagen model peptides, showing that aromatic residues play a role in accelerating the aggregation of triple-helical peptides and affecting their biological activity. The addition of aromatic residues on both ends of a collagen model peptide greatly accelerated the association to higher-order structures as well as affecting morphology. Recent studies by Cejas et al. (*15*, *16*) suggested these effects are mediated largely through end−end aromatic−aromatic interactions, but it is also likely that aromatic residues in one molecule participate in CH···π interactions with imino acids within the triple-helix region of another molecule. The probability of such aromatic−Pro CH···π interactions is supported by the extensive literature on high-resolution globular protein structures, the analysis of the molecular packing in the crystal structure of a triple-helical peptide structure containing a Phe residue, and experimental evidence presented here.

There are detailed analyses of protein structures documenting interactions of aromatic amino acids with Pro residues in proteins, peptides, and complexes (*33*, *35*, *36*). The Cα and Cδ atoms of the Pro ring are adjacent to the backbone amide, making them more acidic and potent hydrogen bond donors. Protons donated by Pro can interact with electron rich aromatic acceptors such as Phe, Tyr, and Trp, leading to CH···π interactions. These CH···π interactions are weaker than those involving strong electron-withdrawing donors such as nitrogen or oxygen but have been shown to contribute 0.5−1.0 kcal/mol to the stability and can play a role in protein folding and function (*33*, *35*, *36*). Hydroxyproline residues would be expected to exhibit similar stabilizing interactions. Although the frequency of these interactions observed in globular proteins increases when the Pro and aromatic residues are close in sequence, there are also well-documented examples in complexes where the Pro is in one polypeptide chain and the aromatic amino acid in another. The high content of both Pro and Hyp on the surface of the collagen triple helix would favor their interactions with available Phe residues in adjacent molecules.

The crystal packing of the collagen integrin binding peptide containing a GFOGER sequence (*29*) provides visualization of molecular details of CH···π intermolecular interactions between an aromatic amino acid in one molecule and imino acids in a neighboring molecule within a triple-helix peptide context. Although it is not possible to draw general conclusions from a single crystal structure, such favorable intermolecular CH···π interactions should be considered when collagen molecules interact with themselves or other proteins containing aromatic residues.

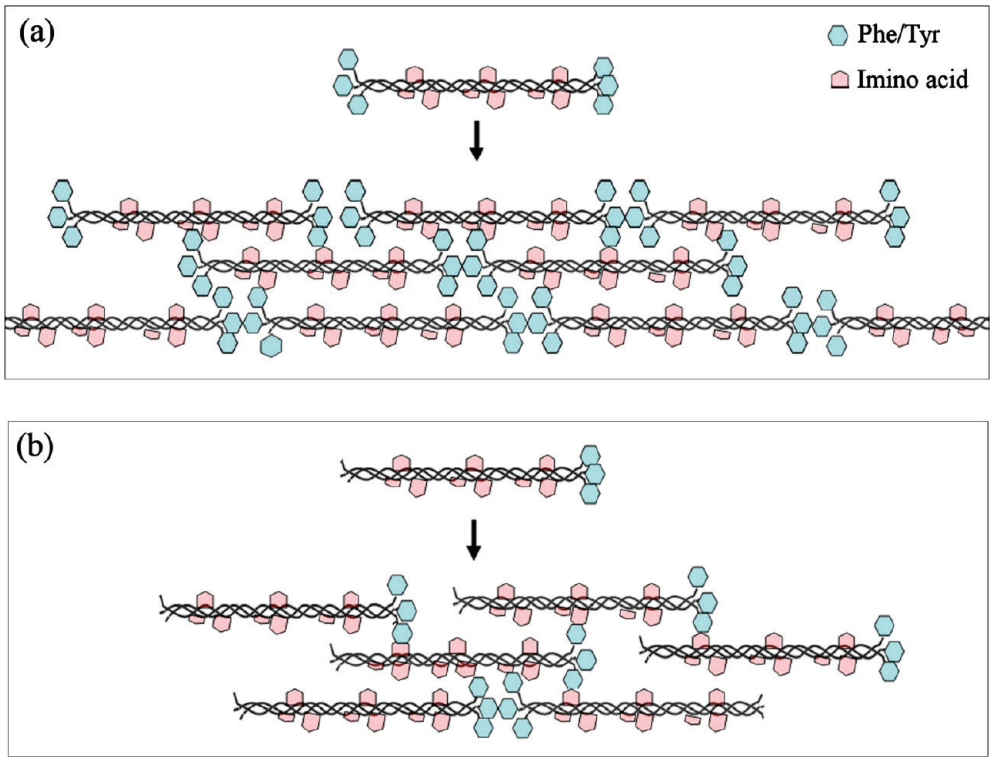

FIGURE 7: Schematic illustration of molecular packing of (a) the FT4Y peptide with aromatic amino acids on both ends of the peptide and (b) the T4Y peptide with an aromatic residue on only the C-terminal end. The $\pi-\pi$ interactions between aromatic residues (blue) on the ends of different molecules are illustrated as well as CH$\cdots\pi$ interactions between aromatic residues (blue) on the peptide termini and imino acids (pink) within the triple helix. The aromatic residues can interact with a number of possible imino acid sites, leading to nonspecific interactions and no periodicity.

The experimental studies reported here are consistent with a role for CH$\cdots\pi$ interactions in the self-association of triple-helical peptides. The increased rate of aggregation and fibril formation of a model triple-helical peptide T4 when there is a Tyr on one end suggests that Tyr may be interacting with Pro/Hyp residues within neighboring triple-helical molecules. Since there are many Pro and Hyp residues in similar sequences within the T4 peptide triple-helix domain, favorable CH$\cdots\pi$ interactions between aromatic residues in the terminus and Pro/Hyp residues in the triple-helix domain of another molecule would be expected to be nonspecific, so the generation of fibrils with no axial periodicity is not surprising (Figure 7). Such nonspecific CH$\cdots\pi$ interactions would still favor nucleation, leading to the observed significant reduction in the lag time of self-assembly and lower critical concentration when one aromatic residue terminates a peptide T4Y. The dramatic acceleration of the rate of self-association when there are aromatic residues on both ends of FT4Y suggests a synergistic effect of $\pi-\pi$ interactions involving aromatic residues on the peptide ends and the CH$\cdots\pi$ interactions between a terminal aromatic residue and imino acids within the neighboring triple helix (Figure 7). The interactions between aromatic residues at the ends of different molecules could lead to long linear fibrils, while nonspecific CH$\cdots\pi$ interactions could promote lateral aggregation.

The presence of CH$\cdots\pi$ interactions between imino acids in the triple helix and aromatic residues is supported by the ability of isolated Phe residues, but not hydrophobic residues, to inhibit the self-association of (Pro-Hyp-Gly)$_{10}$. A strong interaction between Phe and the triple-helical form of the peptide would be expected to lead to an increased stability, but in fact, a small destabilization is observed by DSC when Phe is added to (Pro-Hyp-Gly)$_{10}$. It is possible that Phe is binding to the unfolded as well as the triple-helical state, with somewhat stronger binding to the unfolded peptide. Alternatively, Phe binding could lead to dehydration which would be expected to lower triple-helix stability. It is worth noting that earlier studies suggest the presence of Tyr as a terminal residue can drive the self-assembly process only if the sequence has the intrinsic ability to aggregate (*23*).

The addition of aromatic residues to the T4 peptide modulated molecular association into higher-order structures which influenced their ability to induce platelet aggregation. The ability of soluble and insoluble forms of the FT4Y and T4Y peptides to activate platelets in a dose-dependent manner appears to be related to the presence of a soluble species that has a larger hydrodynamic radius ($R_h \sim 32$ nm) than the single molecule ($R_h \sim 2.5$ nm). Collagen-mediated platelet aggregation is activated through the GPVI receptor, triggering Syk phosphorylation on tyrosine residues 525 and 526 which has been shown to be important for its kinase activity (*31*, *32*). This process is also dependent on positive feedback from thromboxane and secreted ADP. The ability of the FT4Y peptide higher-molecular weight forms to lead to Syk phosphorylation and inhibition by thromboxane inhibitors and ADP receptor antagonists suggests it is acting through the GPVI-mediated pathway. These results suggest even a small aggregate of triple-helical molecules may suffice to interact with GPVI, while a single trimer is not sufficient. The structure of the associated species is important since the aggregated form of (Pro-Hyp-Gly)$_{10}$, which has a clumplike rather than fibrous appearance, has no activity.

Relevance of Aromatic−Imino Acid Residue Interactions to Collagen. The intermolecular aromatic interactions studied in peptides may be relevant to collagen self-association to higher-order structures in tissues. There are few aromatic residues

within the $(Gly\text{-}Xaa\text{-}Yaa)_n$ domain of type I collagen (1.1%), and these are almost exclusively Phe residues, which are found more than 50% of the time in Gly-Phe-Hyp triplets. Fraser et al. (*6*, *14*) reported that a set of Phe residues in type I collagen are concentrated in a short segment in the gap region of D periodic fibrils and suggested this may constitute a stable site within the otherwise flexible gap region. Examination of the sequences of the three major fibril-forming collagens, types I, II, and III, shows that almost all of the Phe residues within the triple helix as well as the aromatic residues within the telopeptides align with a 234-residue periodicity within the collagen molecule in the overlap as well as the gap region, leading to the formation of three or four bands of aromatic amino acids across $D = 670$ Å periodic fibrils (Figure S1 of the Supporting Information). The *D* periodic distribution of Phe residues in fibrillar collagens could lead to $\pi-\pi$ interactions between Phe residues in adjacent molecules within the fibril, but the high frequency of Gly-Phe-Hyp triplets and the proximity of Pro to Phe residues suggest an alternative stabilizing mechanism involving intermolecular Phe−imino contacts such as those seen in the crystal packing of the integrin binding protein. The intermolecular distances and packing symmetry in the integrin binding protein crystal structure resemble collagen molecular packing in fibrils in rat tail tendon as measured by fiber diffraction (*2*, *6*), suggesting that molecular interactions identified in the peptide crystal structure may be biologically relevant.

Fibril-forming collagens contain nonhelical terminal telopeptides which are rich in aromatic amino acids, and the Phe and Tyr residues in telopeptides are highly conserved. Many reports have shown that the telopeptides catalyze collagen fibril formation (*9*−*11*). Synthetic peptides that contain telopeptide sequences inhibit collagen fibrillogenesis, and the aromatic residues in the α2(I) C-telopeptide were shown to be essential for this inhibitory effect (*11*). Prockop and Fertala (*11*) suggested the telopeptides nucleate self-association by binding to a specific region of the central triple helix and that the aromatic residues are essential for this binding. By analogy to the studies on triple-helical peptides, we suggest that favorable $CH\cdots\pi$ interactions between aromatic residues in the telopeptides and Pro/Hyp residues in the triple-helix domain of another molecule could catalyze self-association and fibril formation. In the collagen case, the aromatic residues must interact with a specific site in the adjacent molecule to promote a staggered periodic molecular arrangement, as proposed by Prockop and Fertala (*11*). Such $CH\cdots\pi$ interactions would favor nucleation leading to the observed significant reduction in the lag time of self-assembly and lower critical concentration for acid-extracted collagen when the telopeptides are present compared with pepsin-extracted collagen. The specific nature of the interaction of the telopeptide with the collagen triple helix would also lead to a much lower critical concentration for collagen fibril formation compared with peptide self-association. Consistent with this hypothesis is our observation that addition of Phe (but not Leu or Ala) inhibited fibril formation of pepsin-extracted collagen (personal observation). Less consistent effects were seen for salt-extracted collagen which still retains telopeptides.

The sequence incorporated into the T4 model peptide comes from type IV collagen, where there is a high percentage of Phe residues present largely in Gly-Phe-Hyp triplets as well as in interruptions between the $(Gly\text{-}Xaa\text{-}Yaa)_n$ sequences. It is possible that aromatic−imino acid interactions play a role in the self-association of type IV collagen to the network structure found in basement membranes. Studies also indicate that basement membrane collagen can activate platelet aggregation, and the ability of these type IV model peptides to induce platelet activation could be physiologically significant (*37*, *38*).

Interactions between aromatic residues and Hyp and/or Pro should be considered as factors in promoting self-association of triple helices, in addition to the previously identified roles of the hydration network, hydrogen bonding, and Hyp-mediated interactions (*17*, *39*−*41*). An understanding of the role of aromatic−imino acid interactions in the self-association of triple-helical molecules may provide a tool for understanding the higher-order structure requirement of collagen-activated biological processes such as platelet activation as well as for designing biomaterials and tissue engineering scaffolds.

ACKNOWLEDGMENT

We thank Dr. John Ramsaw for helpful discussions.

SUPPORTING INFORMATION AVAILABLE

Schematic diagram of the amino acid sequences of the three major fibril-forming collagens, types I, II, and III, with a 67 nm, 234-residue stagger, showing the alignment of aromatic residues and the proximity of imino acids (Figure S1). This material is available free of charge via the Internet at http://pubs.acs.org.

REFERENCES

1. Ramachandran, G. N., and Kartha, G. (1955) Structure of collagen. *Nature 176*, 593–595.
2. Bella, J., Eaton, M., Brodsky, B., and Berman, H. M. (1994) Crystal and molecular structure of a collagen-like peptide at 1.9 Å resolution. *Science 266*, 75–81.
3. Rich, A., and Crick, F. H. (1961) The molecular structure of collagen. *J. Mol. Biol. 3*, 483–506.
4. Persikov, A. V., Ramshaw, J. A., and Brodsky, B. (2005) Prediction of collagen stability from amino acid sequence. *J. Biol. Chem. 280*, 19343–19349.
5. Jenkins, C. L., and Raines, R. T. (2002) Insights on the conformational stability of collagen. *Nat. Prod. Rep. 19*, 49–59.
6. Fraser, R. D., MacRae, T. P., and Miller, A. (1987) Molecular packing in type I collagen fibrils. *J. Mol. Biol. 193*, 115–125.
7. Hulmes, D. J., Miller, A., Parry, D. A., Piez, K. A., and Woodhead-Galloway, J. (1973) Analysis of the primary structure of collagen for the origins of molecular packing. *J. Mol. Biol. 79*, 137–148.
8. Farndale, R. W., Lisman, T., Bihan, D., Hamaia, S., Smerling, C. S., Pugh, N., Konitsiotis, A., Leitinger, B., de Groot, P. G., Jarvis, G. E., and Raynal, N. (2008) Cell-collagen interactions: The use of peptide Toolkits to investigate collagen-receptor interactions. *Biochem. Soc. Trans. 36*, 241–250.
9. Helseth, D. L. Jr., and Veis, A. (1981) Collagen self-assembly in vitro. Differentiating specific telopeptide-dependent interactions using selective enzyme modification and the addition of free amino telopeptide. *J. Biol. Chem. 256*, 7118–7128.
10. Kuznetsova, N., and Leikin, S. (1999) Does the triple helical domain of type I collagen encode molecular recognition and fiber assembly while telopeptides serve as catalytic domains? Effect of proteolytic cleavage on fibrillogenesis and on collagen-collagen interaction in fibers. *J. Biol. Chem. 274*, 36083–36088.
11. Prockop, D. J., and Fertala, A. (1998) Inhibition of the self-assembly of collagen I into fibrils with synthetic peptides. Demonstration that assembly is driven by specific binding sites on the monomers. *J. Biol. Chem. 273*, 15598–15604.
12. Kielty, C. M., and Grant, M. E. (2002) The Collagen Family: Structure Assembly and Organization in the Extracellular Matrix. Connective Tissues and Its Heritable Disorders , pp 159−222, Wiley-Liss, New York.
13. Kadler, K. E., Hojima, Y., and Prockop, D. J. (1988) Assembly of type I collagen fibrils de novo. Between 37 and 41 °C the process is limited by micro-unfolding of monomers. *J. Biol. Chem. 263*, 10517–10523.

14. Fraser, R. D., and Trus, B. L. (1986) Molecular mobility in the gap regions of type I collagen fibrils. *Biosci. Rep. 6*, 221–226.
15. Cejas, M. A., Kinney, W. A., Chen, C., Leo, G. C., Tounge, B. A., Vinter, J. G., Joshi, P. P., and Maryanoff, B. E. (2007) Collagen-related peptides: Self-assembly of short, single strands into a functional biomaterial of micrometer scale. *J. Am. Chem. Soc. 129*, 2202–2203.
16. Cejas, M. A., Kinney, W. A., Chen, C., Vinter, J. G., Almond, H. R. Jr., Balss, K. M., Maryanoff, C. A., Schmidt, U., Breslav, M., Mahan, A., Lacy, E., and Maryanoff, B. E. (2008) Thrombogenic collagen-mimetic peptides: Self-assembly of triple helix-based fibrils driven by hydrophobic interactions. *Proc. Natl. Acad. Sci. U.S.A. 105*, 8513–8518.
17. Kar, K., Amin, P., Bryan, M. A., Persikov, A. V., Mohs, A., Wang, Y. H., and Brodsky, B. (2006) Self-association of collagen triple helical peptides into higher order structures. *J. Biol. Chem. 281*, 33283–33290.
18. Kishimoto, T., Morihara, Y., Osanai, M., Ogata, S., Kamitakahara, M., Ohtsuki, C., and Tanihara, M. (2005) Synthesis of poly(Pro-Hyp-Gly)$_n$ by direct poly-condensation of (Pro-Hyp-Gly)$_n$, where $n = 1$, 5, and 10, and stability of the triple-helical structure. *Biopolymers 79*, 163–172.
19. Koide, T., Homma, D. L., Asada, S., and Kitagawa, K. (2005) Self-complementary peptides for the formation of collagen-like triple helical supramolecules. *Bioorg. Med. Chem. Lett. 15*, 5230–5233.
20. Kotch, F. W., and Raines, R. T. (2006) Self-assembly of synthetic collagen triple helices. *Proc. Natl. Acad. Sci. U.S.A. 103*, 3028–3033.
21. Rele, S., Song, Y., Apkarian, R. P., Qu, Z., Conticello, V. P., and Chaikof, E. L. (2007) D-periodic collagen-mimetic microfibers. *J. Am. Chem. Soc. 129*, 14780–14787.
22. Yamazaki, C. M., Asada, S., Kitagawa, K., and Koide, T. (2008) Artificial collagen gels via self-assembly of De Novo designed peptides. *Biopolymers 90*, 816–823.
23. Kar, K., Wang, Y. H., and Brodsky, B. (2008) Sequence dependence of kinetics and morphology of collagen model peptide self-assembly into higher order structures. *Protein Sci. 17*, 1086–1095.
24. Morton, L. F., Hargreaves, P. G., Farndale, R. W., Young, R. D., and Barnes, M. J. (1995) Integrin $\alpha 2\beta 1$-independent activation of platelets by simple collagen-like peptides: Collagen tertiary (triple-helical) and quaternary (polymeric) structures are sufficient alone for $\alpha 2\beta 1$-independent platelet reactivity. *Biochem. J. 306* (Part 2), 337–344.
25. Smethurst, P. A., Onley, D. J., Jarvis, G. E., O'Connor, M. N., Knight, C. G., Herr, A. B., Ouwehand, W. H., and Farndale, R. W. (2007) Structural basis for the platelet-collagen interaction: The smallest motif within collagen that recognizes and activates platelet glycoprotein VI contains two glycine-proline-hydroxyproline triplets. *J. Biol. Chem. 282*, 1296–1304.
26. Jarvis, G. E., Raynal, N., Langford, J. P., Onley, D. J., Andrews, A., Smethurst, P. A., and Farndale, R. W. (2008) Identification of a major GpVI-binding locus in human type III collagen. *Blood 111*, 4986–4996.
27. Gill, S. C., and von Hippel, P. H. (1989) Calculation of protein extinction coefficients from amino acid sequence data. *Anal. Biochem. 182*, 319–326.
28. Persikov, A. V., Xu, Y., and Brodsky, B. (2004) Equilibrium thermal transitions of collagen model peptides. *Protein Sci. 13*, 893–902.
29. Emsley, J., Knight, C. G., Farndale, R. W., and Barnes, M. J. (2004) Structure of the integrin $\alpha 2\beta 1$-binding collagen peptide. *J. Mol. Biol. 335*, 1019–1028.
30. Kahner, B. N., Shankar, H., Murugappan, S., Prasad, G. L., and Kunapuli, S. P. (2006) Nucleotide receptor signaling in platelets. *J. Thromb. Haemostasis 4*, 2317–2326.
31. Farndale, R. W., Sixma, J. J., Barnes, M. J., and de Groot, P. G. (2004) The role of collagen in thrombosis and hemostasis. *J. Thromb. Haemostasis 2*, 561–573.
32. Nieswandt, B., and Watson, S. P. (2003) Platelet-collagen interaction: Is GPVI the central receptor?. *Blood 102*, 449–461.
33. Brandl, M., Weiss, M. S., Jabs, A., Suhnel, J., and Hilgenfeld, R. (2001) C-H$\cdots\pi$-interactions in proteins. *J. Mol. Biol. 307*, 357–377.
34. Hunter, C. A., Singh, J., and Thornton, J. M. (1991) π-π interactions: The geometry and energetics of phenylalanine-phenylalanine interactions in proteins. *J. Mol. Biol. 218*, 837–846.
35. Bhattacharyya, R., and Chakrabarti, P. (2003) Stereospecific interactions of proline residues in protein structures and complexes. *J. Mol. Biol. 331*, 925–940.
36. Steiner, T., and Koellner, G. (2001) Hydrogen bonds with π-acceptors in proteins: Frequencies and role in stabilizing local 3D structures. *J. Mol. Biol. 305*, 535–557.
37. Henrita, G., Saelman, E. U., Schut-Hese, K. M., Wu, Y. P., Slootweg, P. J., Nieuwenhuis, H. K., de Groot, P. G., and Sixma, J. J. (1996) Platelet adhesion to collagen type IV under flow conditions. *Blood 88*, 3862–3871.
38. Polanowska-Grabowska, R., Simon, C. G. Jr., and Gear, A. R. (1999) Platelet adhesion to collagen type I, collagen type IV, von Willebrand factor, fibronectin, laminin and fibrinogen: Rapid kinetics under shear. *Thromb. Haemostasis 81*, 118–123.
39. Leikin, S., Parsegian, V. A., Yang, W., and Walrafen, G. E. (1997) Raman spectral evidence for hydration forces between collagen triple helices. *Proc. Natl. Acad. Sci. U.S.A. 94*, 11312–11317.
40. Leikin, S., Rau, D. C., and Parsegian, V. A. (1995) Temperature-favoured assembly of collagen is driven by hydrophilic not hydrophobic interactions. *Nat. Struct. Biol. 2*, 205–210.
41. Vitagliano, L., Berisio, R., Mazzarella, L., and Zagari, A. (2001) Structural bases of collagen stabilization induced by proline hydroxylation. *Biopolymers 58*, 459–464.